Magneto-optical absorption in a one-dimensional array of narrow antiwires

Danhong Huang
Department of Electrical & Computer Engineering, Wayne State University, Detroit, Michigan 48202

Godfrey Gumbs*
Department of Physics and Astronomy, Hunter College of the City University of New York, 695 Park Avenue, New York, New York 10021

Norman J. M. Horing
Department of Physics and Engineering Physics, Stevens Institute of Technology, Castle Point on the Hudson, Hoboken, New Jersey 07030

(Received 12 November 1993)

We present a self-consistent field theory for the infrared absorption coefficient of an array of narrow antiwires in a perpendicular external magnetic field. A detailed study is made of the way in which the collective mode changes from a cyclotron mode when the confining potential is weak to tunneling coupled modes for intermediate antiwire potential strength and then to edge and one-dimensional lattice magnetoplasmon modes for strong potentials. Our numerical calculations show that at low magnetic fields, there is appreciable electron tunneling between quantum wires. However, as the magnetic field is increased, the electron tunneling is suppressed. The suppression of electron tunneling between wires is observed when the tunneling coupled modes emerge into cyclotron modes in the strong magnetic field regime. The edge mode excitation energy oscillates as a function of the electron density. These oscillations correspond to soft or hard potential walls for which the electron states are extended and localized, respectively.

Experimental observations such as the quantum Hall effect[1] in the two-dimensional electron gas (2DEG), the quenching of the Hall effect in quantum wire junction[2] and antidots,[3–5] the quantization of the resistance of ballistic point contacts,[6] and the optical properties of quantum wires[7] have led to an intense investigation of the optical and transport properties of systems of reduced dimensionality. Experiments have also dealt with related systems such as quantum rings.[8] Strong periodic modulations and mutual Coulomb scattering have produced novel effects in the 2DEG subject to one-dimensional (1D) (Ref. 9) or 2D (Ref. 10) electric potential modulation.

Recently, submicrometer lithographic technology has been used to produce quantum wires which contain a number of electrons in discrete energy subbands. The *reversed structure* to wires is antiwires which are obtained by etching an array of microscopic grooves of submicrometer width into a high mobility 2DEG conductor.[11] The introduction of this strong spatially modulated potential leads to dramatic commensurability effects at low temperature in uniform external magnetic fields. In this array of artificial scatterers, there is pronounced structure in the magnetoresistance. Hansen *et al.*[7] reported the observation of a softened magnetoplasmon mode by varying the gate voltage. Wulf *et al.*[12] and Gumbs *et al.*[13] proposed explanations to this softening behavior, separately. Demel *et al.*[14] observed the 1D magnetoplasmons in an array of multiple quantum wires where both the edge and Coulomb coupled modes were found in infrared absorption experiments. Goñi *et al.*[15] further discovered rotons and spin-flip excitations in such a system by using light scattering. The same structure also showed oscillations in the longitudinal conductance as a function of an applied gate voltage due to the successive population of the 1D subbands. For 1D and 2D magnetic field modulations, Schmidt[16] and Xue and Xiao[17] calculated the deterministic diffusion and magnetotransport. In 1D lateral quantum wire superlattices in the weak modulation limit, Gerhardts and and co-workers[18] theoretically investigated the magnetotransport in which the commensurability oscillations in the longitudinal conductivity were explained as being due to the changes in the Landau band arising from the 1D potential modulation when localized and extended states are formed by the magnetic field. Cui *et al.*[19] calculated the magnetoplasmon excitation in the same 1D lateral superlattices where the commensurability oscillations were predicted in the magnetic field dispersion of the excitation energy. Wulf *et al.*[9] studied the magnetotransport in the strong modulation limit where giant oscillations in the Hall conductivity were observed.

Although there have already been some experimental and theoretical studies for the 1D array of quantum wires, only a few deal with the infrared absorption and magnetotransport in the 1D array of antiwires. The physics in a very weak modulation limit can be well understood on the basis of a first-order perturbation theory. However, the lack of self-consistency by taking the zero-order wave function[18,19] completely excludes the effect from the lattice periodicity. In the very strong modulation limit, the system can be viewed as a 1D lattice since the small effect from the magnetic quantization is negligible in this case. What is unknown turns out to be the physics in the intermediate modulation regime where the Landau and size quantization becomes comparable to each other. The cyclotron mode in the 2DEG is split into the tunneling coupled modes in the weak modulation regime. In

0163-1829/94/49(16)/11463(4)/$06.00

the crossover regime, these two coupled modes gradually develop into the edge and 1D lattice magnetoplasmon modes in the strong modulation regime.

In this paper, we present a model for an array of narrow antiwires and a self-consistent field theory for the infrared absorption coefficient. We carry out a detailed calculation of the infrared absorption spectra as a function of the antiwire modulation strength, the magnetic field, and the electron density.

The single-particle Hamiltonian for a 1D periodic array of narrow antiwires in the x-y plane in a uniform perpendicular magnetic field $\mathbf{B}$ is given in the Landau gauge by

$$\mathcal{H}_0 = \frac{1}{2m^*}\left[-\hbar^2\frac{\partial^2}{\partial x^2} + \left(\frac{\hbar}{i}\frac{\partial}{\partial y} + eBx\right)^2\right] + V^{\rm ext}(x) \ , \quad (1)$$

where m^* is the electron effective mass. In Eq. (1), the narrow antiwire potential $V^{\rm ext}(x)$ is taken as one-dimensional δ functions

$$V^{\rm ext}(x) = V_0 \sum_{m=-\infty}^{\infty} \delta(x - ma) \ , \quad (2)$$

where $V_0/a > 0$ represents the strength of the antiwire potential. The approximate form in Eq. (2) for simulating a 1D array of narrow antiwires reduces the amount of numerical calculations considerably. Furthermore, this model is satisfactory provided that the lattice period a is much larger than the widths of the antiwires.

In the presence of the antiwire potential, the single-particle energy eigenstates are labeled by the quantum numbers $(j,\ X_0)$ and we expand the eigenfunctions according to

$$\psi_{j,X_0}(x,\ y) = \sum_{n=0}^{\infty} C_n(j, X_0)\ \phi_{n,X_0}(x,\ y) \ , \quad (3)$$

where $\phi_{n,X_0}(x,\ y)$ are harmonic oscillator wave functions for a homogeneous 2DEG, with energy eigenvalues $E_n^{(0)} = (n + 1/2)\hbar\omega_c$. Here, $\omega_c = eB/m^*$ is the cyclotron frequency. In this notation, $n = 0,\ 1,\ 2,\ \ldots$ is a Landau-level index, $X_0 = k_y L_H^2$ is the guiding center, k_y is the wave vector along the y direction, and $L_H = (\hbar/eB)^{1/2}$ is the magnetic length. The expansion coefficients $C_n(j,\ X_0)$ in Eq. (3) are determined from the following linear equation:

$$\sum_{n=0}^{\infty}\{[E_n^{(0)} - E_j(X_0)]\delta_{n,n'} + B_{n',n}(X_0)\}C_n(j,\ X_0) = 0 \ , \quad (4)$$

as well as the orthonormality condition: $\sum_{n=0}^{\infty} C_n(j,\ X_0)C_n(j',\ X_0) = \delta_{j,j'}$. We obtain a secular equation for the jth energy eigenvalue $E_j(X_0)$ by setting the determinant of the coefficient matrix in Eq. (4) equal to zero. Also, the second term in the coefficient matrix in Eq. (4) is given by

$$B_{n',n}(X_0) = V_0 \sum_{l=-\infty}^{\infty} (1/\pi 2^{(n+n')}n!n'!L_H^2)^{1/2} \times e^{-(la+X_0)^2/L_H^2}\ H_n[(la + X_0)/L_H] \times H_{n'}[(la + X_0)/L_H] \ , \quad (5)$$

where $H_n(x)$ is the nth order Hermite polynomial. Clearly, $B_{n',n}(X_0)$ has the periodicity of the lattice. From this, it follows from Eq. (5) that $E_j(X_0) = E_j(X_0 + a)$. Since the coefficient matrix in Eq. (4) is real and symmetric, $C_n(j,\ X_0)$ must be real.

A straightforward but lengthy calculation yields the Lorentz ratio $\alpha_L(\omega)$ defined as the ratio of the Fourier coefficient of the absorbed energy of frequency ω of an external electric field to the square of the amplitude of the probing field. We have

$$\alpha_L(\omega) = -\frac{e^2 A}{\pi L_H^2}\sum_{j\neq j'}\int_0^a \frac{dX_0}{a} X_{j,j'}(X_0) \times\left[\frac{f_0\,[E_j(X_0)] - f_0\,[E_{j'}(X_0)]}{\hbar\omega - [E_{j'}(X_0) - E_j(X_0)] + i\gamma}\right] \times\left[X_{j,j'}(X_0) + \sum_{m=-\infty}^{\infty}\left(\frac{\delta\rho_{\rm ind}(mG;\ \omega)}{eE^{\rm ext}}\right) \times S(|mG|)F_{j,j';X_0}(mG)\ e^{imGX_0}\right] . \quad (6)$$

In this notation, A is the area of the sample, γ is the optical broadening due to impurity, phonon, and surface roughness scattering, $E^{\rm ext}$ is the amplitude of the probing field, $G = 2\pi/a$ is a reciprocal lattice vector, and $f_0[E_j(X_0)] = \{1+\exp[E_j(X_0)-E_F]/k_BT\}^{-1}$ is the Fermi distribution function; E_F is the Fermi energy determined by the electron density $n_{\rm 2D}$. The dipole transition matrix $X_{j,j'}(X_0)$ is given by

$$X_{j,j'}(X_0) = \frac{L_H}{\sqrt{2}}\sum_{n=0}^{\infty} C_n(j,\ X_0)[\sqrt{n+1}C_{n+1}(j',\ X_0) + \sqrt{n}C_{n-1}(j',\ X_0)] - X_0\delta_{j,j'} \ , \quad (7)$$

and the form factor is defined by

$$F_{j,j';X_0}(mG) = \sum_{n,n'=0}^{\infty} C_n(j,\ X_0)C_{n'}(j',\ z_0) \times[\sqrt{N_<!/N_>!}\ [i\ \mathrm{sgn}\ (-m)]^{(N_>-N_<)} \times e^{-m^2G^2L_H^2/4}(m^2G^2L_H^2/2)^{(N_>-N_<)/2} \times L_{N_<}^{(N_>-N_<)}(m^2G^2L_H^2/2)] \ , \quad (8)$$

where $\mathrm{sgn}(x)$ is the signum function, $L_n^m(x)$ is a Laguerre polynomial, $N_< = \min\{n,\ n'\}$, and $N_> = \max\{n,\ n'\}$. The screened factor of Coulomb interaction due to the finite thickness L_z of the EG layer has been calculated as

$$S(|mG|) = \frac{2\pi e^2}{\epsilon_s|m|G}\left[\frac{8 + 9|m|GL_z + 3m^2G^2L_z^2}{8(1 + |m|GL_z)^3}\right] \ , \quad (9)$$

where $\epsilon_s \equiv 4\pi\epsilon_0\epsilon_b$ and ϵ_b is the background dielectric constant. In Eq. (9), the Fang-Howard variational ground state wave function in the z direction for a 2D heterojunction was used. In Eq. (6), the induced electron density is a solution of the following linear equation:

$$\sum_{m=-\infty}^{\infty}[\delta_{m',m} - A_{m',m}(\omega)]\left(\frac{\delta\rho_{\rm ind}(mG;\ \omega)}{eE^{\rm ext}}\right) = R_{m'}(\omega), \quad (10)$$

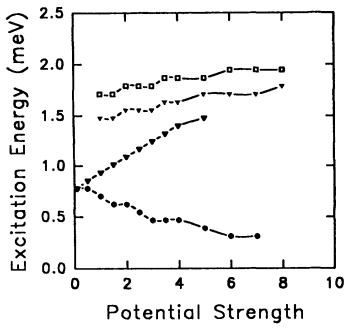

FIG. 1. The excitation energies of edge mode (filled circle), cyclotron mode (unfilled triangle), and 1D lattice magnetoplasmon modes (filled triangle and unfilled square) are shown as a function of the antiwire potential $\bar{V} = (V_0/a)/(\sqrt{\pi}\hbar^2/m^*a^2)$. The parameters in the numerical calculation are chosen as follows: $a = 1000$ Å, $m^* = 0.067m_e$, $\epsilon_b = 12.9$, $L_z = 50$ Å, $\gamma = 0.12$ meV, $T = 0$ K, $B = 0.45$ T, $n_{2D}a^2 = 5.0$.

where

$$A_{m',m}(\omega) = \frac{1}{2\pi L_H^2}\sum_{j\neq j'}\int_0^a \frac{dX_0}{a} F^*_{j,j';X_0}(m'G) \times F_{j,j';X_0}(mG)S(|mG|)e^{i(m-m')GX_0} \times \frac{f_0[E_j(X_0)] - f_0[E_{j'}(X_0)]}{\hbar\omega - [E_{j'}(X_0) - E_j(X_0)] + i\gamma} \quad (11)$$

and

$$R_m(\omega) = \frac{1}{2\pi L_H^2}\sum_{j\neq j'}\int_0^a \frac{dX_0}{a} F^*_{j,j';X_0}(mG)e^{-imGX_0} \times X_{j,j'}(X_0)\left[\frac{f_0[E_j(X_0)] - f_0[E_{j'}(X_0)]}{\hbar\omega - [E_{j'}(X_0) - E_j(X_0)] + i\gamma}\right]. \quad (12)$$

The absorption coefficient is given in terms of the real (Re) and the imaginary (Im) parts of the Lorentz ratio by[20]

$$\beta_{\rm abs}(\omega) = [\omega/\epsilon_0 c L_z A n_r(\omega)]\,[\rho_{\rm ph}(\omega) + 1]\,{\rm Im}\alpha_L(\omega)\ , \quad (13)$$

where $\rho_{\rm ph}(\omega) = [\exp(\hbar\omega/k_BT) - 1]^{-1}$ is the photon distribution function, and the frequency-dependent refractive index is

$$n_r(\omega) = \left(\tfrac{1}{2}\{\epsilon_b + {\rm Re}\alpha_L(\omega)/\epsilon_0 L_z A + \sqrt{[\epsilon_b + {\rm Re}\alpha_L(\omega)/\epsilon_0 L_z A]^2 + [{\rm Im}\alpha_L(\omega)/\epsilon_0 L_z A]^2}\ \}\right)^{1/2}. \quad (14)$$

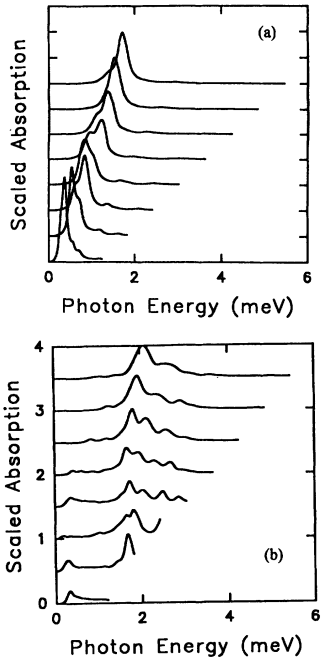

FIG. 2. Plots of the absorption coefficient $\beta_{\rm abs}(\omega)a$ as a function of the photon energy $\hbar\omega$ for various values of the magnetic field B in the intermediate [$\bar{V} = 1.0$ in (a)] and the strong [$\bar{V} = 5.0$ in (b)] potential modulation regimes. The parameters in the calculation are the same as those in Fig. 1. Each curve in the figures is shifted upward by a constant. From the bottom, the curves correspond to $B = 0.2 - 0.9$ in steps of 0.1 T.

Figure 1 shows plot of resonant peak positions of the absorption coefficient as a function of the antiwire potential strength. This is an example that shows how the magnetoplasmon mode changes from a cyclotron mode in the weak modulation potential regime to a 1D lattice magnetoplasmon mode when the modulation potential is strong. For intermediate values of the lattice potential, the cyclotron mode first splits into two new tunneling coupled modes. One of these two coupled modes develops into the 1D lattice magnetoplasmon mode when the lattice potential becomes strong while the other gradually changes into an edge mode as the potential strength is increased. The antiwire potential first shifts the electron energy levels upward which enhance the electron tunneling from both sides of the antiwire. However, when the potential is very strong so that the electron tunneling is suppressed, we are left with an array of isolated wide quantum wires. The potential strength dispersion of the tunneling coupled modes is appreciable compared with the 1D lattice magnetoplasmon modes. When the modulation potential becomes strong, a hard potential wall is formed which favors the electrons performing skipping orbits along the wall. As a consequence, the excitation energy of the edge mode decreases as the potential is increased. In the weak potential regime, the tunneling coupled modes are the dominant excitations. Whereas in the strong potential regime, the 1D lattice magnetoplasmon mode becomes dominant. There is a crossover region where the absorption peaks of both of these modes are comparable.

Figures 2(a) and 2(b) are plots of the absorption coefficient as a function of the photon energy for various values of the magnetic field in the intermediate [Fig. 2(a)] and the strong [Fig. 2(b)] modulation potential regimes. Fig-

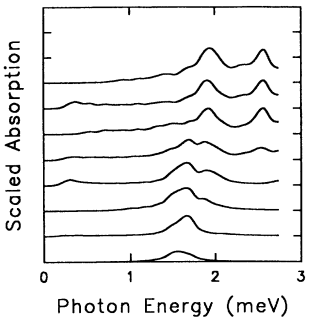

FIG. 3. Calculated absorption coefficient $\beta_{\rm abs}(\omega)a$ is shown as a function of the photon energy $\hbar\omega$ for various values of the electron density $n_{2D}a^2$ in the strong potential modulation regime with $\bar{V} = 5.0$. The parameters in the calculation are the same as those in Fig. 1. Each curve in the figure is shifted upward by a constant. From the bottom, the curves correspond to $n_{2D}a^2 = 1.0 - 8.0$ in steps of 1.0.

ure 2(a) shows the crossover from the tunneling coupled modes at weak magnetic fields to the cyclotron mode at strong magnetic fields. During this process, there are significant peak strength exchanges between the tunneling coupled modes which correspond to antiphase oscillations in the peak strengths as a function of the magnetic field for these two modes. The $2\hbar\omega_c$ and the $3\hbar\omega_c$ modes are also visible at low magnetic fields because of the broken translational symmetry in the system. On the other hand, in the strong potential regime, as in Fig. 2(b), we can see the crossover from a 1D lattice magnetoplasmon and edge modes at weak magnetic field to the cyclotron mode at even higher magnetic fields, after passing through the formation of tunneling coupled modes.

Figure 3 shows the calculated absorption coefficient as a function of photon energy for various values of the electron density in the strong modulation potential regime. The edge mode oscillates as a function of the electron density. When the Fermi energy lies about halfway between two Landau bands, corresponding to localized states, the excitation energy is a minimum. In this case, the potential wall of the antiwires is comparatively hard which favors skipping orbits of the electrons. When the Fermi energy is within a Landau band, corresponding to the extended states, the edge mode excitation has the maximum energy. Here, the potential wall becomes soft and the coupling between both sides of the antiwire shifts the excitation energy upward.

Compared to the 1D array of narrow quantum wires with $V_0 < 0$ (not shown here), we find that the absorption strength in this case is four times smaller. This is because most of the electrons are located outside the narrow quantum wires. This is a result of electron overflowing due to the elevated energy levels by the strong electrostatic confinement.

In conclusion, we have used δ potentials to simulate an array of narrow antiwires. We have derived a self-consistent field theory for the infrared absorption of this system. The crossover of the cyclotron mode to two tunneling coupled modes and finally to the edge and 1D lattice magnetoplasmon modes with the increase of antiwire potential is thoroughly studied. The magnetic field enhanced and suppressed electron tunneling, associated with the evolutions to cyclotron mode at strong magnetic field passing through the formation of tunneling coupled modes are observed. The edge mode excitation energy oscillates as a function of the electron density. These oscillations correspond to a soft or hard potential wall for which the electron states are extended and localized, respectively.

The authors gratefully acknowledge the support in part from the City University of New York PSC-CUNY-BHE Grant No. 662505 and Office of Naval Research under Contract No. N00014-93-1-0576. Critical comments by H. L. Cui, V. Fessatidias, A. H. MacDonald, and M. Pepper are gratefully acknowledged.

* Also at The Graduate School and University Center, City University of New York, 33 West 42 Street, New York, NY 10036.

[1] K. von Klitzing, G. Dorda, and M. Pepper, Phys. Rev. Lett. **45**, 494 (1980).
[2] M. L. Roukes *et al.*, Phys. Rev. Lett. **59**, 3011 (1987).
[3] D. Weiss, K. von Klitzing, K. Ploog, and G. Weimann, Europhys. Lett. **8**, 179 (1989); see also, *High Magnetic Fields in Semiconductor Physics II*, edited by G. Landwehr, Springer Series in Solid State Sciences Vol. 87 (Springer-Verlag, Berlin, 1989), p. 357.
[4] D. Weiss *et al.*, Phys. Rev. Lett. **70**, 4118 (1993).
[5] E. S. Alves *et al.*, J. Phys. Condens. Matter **1**, 8257 (1989).
[6] B. J. van Wees *et al.*, Phys. Rev. Lett. **60**, 848 (1988).
[7] W. Hansen, M. Horst, J. P. Kotthaus, U. Merkt, C. Sikorski, and K. Ploog, Phys. Rev. Lett. **58**, 2586 (1987).
[8] R. A. Webb, S. Washburn, C. Umbach, and R. A. Laibowitz, Phys. Rev. Lett. **54**, 2696 (1985).
[9] U. Wulf, J. Kučera, and A. H. MacDonald, Phys. Rev. B **47**, 1675 (1993).
[10] C. G. Smith, M. Pepper, R. Newbury, H. Ahmed, D. G. Hasko, D. C. Peacock, J. E. F. Frost, D. A. Ritchie, G. A. C. Jones, and G. Hill, J. Phys. Condens. Matter **2**, 3405 (1990); C. G. Smith, W. Chen, M. Pepper, H. Ahmed, D. G. Hasko, D. A. Ritchie, J. E. F. Frost, and G. A. C. Jones, J. Vac. Sci. Technol. B **10**, 2904 (1992).
[11] G. M. Gusev, P. Basmaji, Z. D. Kvon, L. V. Litvin, Y. V. Nastaushev, and A. I. Toropov, Solid State Commun. **85**, 317 (1993).
[12] U. Wulf, E. Zeeb, P. Gies, R. R. Gerhardts, and W. Hanke, Phys. Rev. B **41**, 3113 (1990); **42**, 7637 (1990).
[13] G. Gumbs, D. Huang, and D. Heitmann, Phys. Rev. B **44**, 8084 (1991).
[14] T. Demel, D. Heitmann, P. Grambow, and K. Ploog, Phys. Rev. Lett. **66**, 2657 (1991).
[15] A. R. Goñi, A. Pinczuk, J. S. Weiner, B. S. Dennis, L. N. Pfeiffer, and K. W. West, Phys. Rev. Lett. **70**, 1151 (1993).
[16] Götz J. O. Schmidt, Phys. Rev. B **47**, 13 077 (1993).
[17] D. P. Xue and G. Xiao, Phys. Rev. B **45**, 5986 (1992).
[18] R. R. Gerhardts, D. Weiss, and K. von Klitzing, Phys. Rev. Lett. **62**, 1173 (1989); R. R. Gerhardts and C. Zhang, *ibid.* **64**, 1473 (1990).
[19] H. L. Cui, V. Fessatidis, and N. J. M. Horing, Phys. Rev. Lett. **63**, 2598 (1989).
[20] A. Haug, *Theoretical Solid State Physics* (Pergamon, New York, 1972), Vol. 1, p. 360.